JCTC Journal of Chemical Theory and Computation

ARTICLE

pubs.acs.org/JCTC

Structures, Energetics, and IR Spectra of Monohydrated Inorganic Acids: Ab initio and DFT Study

Maciej Kołaski,[†,‡] Aleksey A. Zakharenko,[†] S. Karthikeyan,[†] and Kwang S. Kim[*,†]

[†]Center for Superfunctional Materials, Department of Chemistry, Pohang University of Science and Technology, San 31, Hyojadong, Namgu, 790-784 Pohang, South Korea

S Supporting Information

ABSTRACT: We carried out extensive calculations of diverse inorganic acids interacting with a single water molecule, through a detailed analysis of many possible conformations. The optimized structures were obtained by using density functional theory (DFT) and the second order Møller−Plesset perturbation theory (MP2). For the most stable conformers, we calculated the interaction energies at the complete basis set (CBS) limit using coupled cluster theory with single, double, and perturbative triple excitations [CCSD(T)]. The −OH stretching harmonic and anharmonic frequencies are provided as fingerprints of characteristic conformers. The zero-point energy (ZPE) uncorrected/corrected ($\Delta E_e/\Delta E_0$) interaction energies and the enthalpies/free energies ($\Delta H_r/\Delta G_r$ at room temperature and 1 bar) are reported. Various comparisons are made between many diverse inorganic acids (H_mXO_n where X = B/N/P/Cl/Br/I, $m = 1-3$, and $n = 0-4$) as well as other simple inorganic acids. In many cases, we find that the dispersion-driven van der Waals interactions between X in inorganic acid molecules and O in water molecules as well as the $X^+\cdots O^-$ electrostatic interactions are important.

INTRODUCTION

The hydration phenomena of diverse molecular systems including cations,[1] anions,[2] simple acids[3]/bases,[4] and salts[5] have been reported. However, the structures, spectra, and thermochemical data for hydration of a large family of inorganic acids with boron, nitrogen, phosphorus, and sulfur atoms as well as halide atoms are still scarce.[6] Thus, we are interested in studying the hydration of such inorganic acids: HBO_2/HBO_3, HNO_2/HNO_3, H_3PO_3/ H_3PO_4, H_2SO_3/H_2SO_4, H_2S, H_2Se, HCN, HF, $HClO_{n=0-4}$, $HBrO_{n=0-4}$, and $HIO_{n=0-4}$. However, due to high complexity of the hydration/dehydration phenomena which requires extensive studies, the present aim is not to study such complex phenomena, but we have tried to investigate the monohydrated inorganic acids as the first step toward understanding hydration of the above 27 inorganic acids. The information from various monohydrated inorganic acids would be useful in studying both protonated acid cations and deprotonated acid anions.

We begin with brief introduction of various inorganic acids studied here. HCl, HBr, HI, and HNO_3 are strong monoprotic acids, and H_2SO_4 is a biprotic strong acid. H_3BO_3 and H_3PO_4 are weak triprotic acids. Hypochlorous (HClO), hypobromous (HBrO), and hypoiodous (HIO) acids are the simplest examples of weak acids. Chlorous ($HClO_2$), bromous ($HBrO_2$), and iodous (HIO_2) acids are also relatively weak in comparison with other inorganic acids. Chloric acid ($HClO_3$) is known as a strong acid and a very efficient oxidizing agent. Iodic acid (HIO_3) exists as a white solid and is insoluble in water, unlike chloric and bromic acids. Perchloric acid ($HClO_4$) is a strong acid which completely dissociates in an aqueous solution. Its strength is comparable to sulfuric acid (H_2SO_4) and nitric acid (HNO_3). Perbromic acid ($HBrO_4$) is a strong acid and an important oxidizing agent in many chemical reactions. Periodic acid (HIO_4) is widely employed in organic chemistry for structural analysis. Periodic acid can cleave a vicinal diol into two aldehyde or ketone fragments, which is useful in determining the structure of carbohydrates.

The nitric acid (HNO_3)[7−17] and sulfuric acid (H_2SO_4)[18−25] were widely studied theoretically. Owing to experimental difficulties, less attention is paid to sulfurous acid [H_2SO_3 or $HS(OH)O_2$],[26,27] while little is known about sulfonic acid [$(HO)_2SO$] which has the same chemical formula. The sulfur-containing acid with the simplest chemical formula H_2S (hydrogen sulfide) is a covalent hydride related structurally to the water molecule, since oxygen and sulfur belong to the same group of the periodic table of elements.[28,29] Hydrogen selenide (H_2Se) is the simplest hydride of selenium, a colorless flammable gas under standard conditions, and soluble in water. The physicochemical properties of H_2S and H_2Se are similar.

The phosphoric acid (H_3PO_4) is used as the electrolyte in fuel cells, and the phosphorous acid (H_3PO_3; $HP(OH)_2O$] is commonly used as oxoacids of phosphorus.[30−34] As in H_2SO_3, the isomer $P(OH)_3$ is not known well, like sulfonic acid $(HO)_2SO$. Phosphoric acid may be used as a "rust converter", by direct application to rusted iron, steel tools, or surfaces. The hydrogen cyanide (HCN) is a valuable precursor to many chemical compounds ranging from polymers to pharmaceuticals. Hydrogen cyanide is a colorless, very poisonous, and highly volatile liquid that boils slightly above room temperature at 26 °C.[35−37] It is important to note that HCN is one of the simplest cyanide systems which can act as both proton donor and acceptor.

In this work, we compare the interaction energies, H-bond lengths (r_{OH}), natural bond orbital (NBO) charges (q), and −OH IR (infrared) stretching harmonic/anharmonic vibrational frequencies (ν_s) using DFT and extensive high-level ab initio

Received: August 2, 2010
Published: August 25, 2011

calculations of diverse inorganic acids interacting with a single water molecule.

COMPUTATIONAL DETAILS

We have carried out geometry optimization, harmonic/anharmonic frequency analysis, and calculated interaction energies for many different monohydrated inorganic acids. Geometry optimization and harmonic frequency calculations were done at the DFT level of theory employing Becke's three-parameter exchange potential and the Lee−Yang−Parr correlation functional (B3LYP) as well as second order Møller−Plesset perturbation (MP2) theory. The anharmonic frequencies were obtained at the MP2 level of theory. Calculations were carried out by using the Gaussian 03 suite of programs.[38] The zero-point energy correction is only the second order for the anharmonic terms, and so this anharmonic correction is insignificant in general. The thermal energy corrections are calculated based on rigid rotor and harmonic oscillator approximation. Throughout the present work, all the atoms were treated with the aug-cc-pVDZ basis set (which we have abbreviated as aVDZ) and the aug-cc-pVTZ basis set (which will be abbreviated as aVTZ). Since the aVDZ/aVTZ basis set is not available for iodine, the CRENBL ECP basis set was employed. This basis set uses relativistic effective core potentials and an extended valence basis set. Since only one CRENBL ECP basis set alone cannot be exploited for the basis set extrapolation to estimate the complete basis set (CBS) limit energy (even though all atoms are treated with aVDZ and aVTZ basis sets), the reported CBS energies for iodine-containing clusters are approximate in that the extrapolation related to the I atom is not properly taken into account. All optimized structures were drawn with the Posmol package.[39] To obtain more reliable results, we carried out single point coupled cluster theory with single, double, and perturbative triple excitations [CCSD(T)] calculations for the most stable conformers of monohydrated acids. To estimate the CCSD(T)/CBS interaction energies, we obtain the CBS limit values for the MP2 interaction energies using the extrapolation method exploiting that the basis set error in the electron correlation energy is proportional to N^{-3} for the aug-cc-pVNZ (which we have abbreviated as aVNZ) basis set (aVDZ for $N = 2$, aVTZ for $N = 3$).[40,41] Given that the difference in interaction energy between MP2/aVNZ and CCSD(T)/aVNZ does not differ significantly with increasing size of the basis set, the CCSD(T)/CBS interaction energies are evaluated from the MP2/CBS ones by using the difference between CCSD(T)/aVDZ and MP2/aVDZ interaction energies.[41,42] The CCSD(T) calculations were carried out by using the MOLPRO suite of programs.[43] Then, these interaction energies (ΔE_e) are used to evaluate the zero-point energy (ZPE) corrected interaction energies (ΔE_0) and the enthalpy and Gibbs free energies at room temperature (298.15 K) and 1 bar, by using the MP2/aVDZ ZPEs and thermal energies.

All the reported structures are at the local or global minima without imaginary frequencies. All structures found for one type of acid···water clusters were attempted for all similar monohydrated inorganic acids. To distinguish different conformers, we use the following notation: A_Y/D_Z denotes the role of proton acceptor (A: O)/donor (D: H) by the water molecule, while the subscript "$_{Y/Z}$" denotes the atom of each acid interacting with the O/H atom of H_2O. Since $A_{H(O)}$ is the most common case, it will be simply denoted as A, which is distinguished from $A_{H(X)}$ to be simply denoted A_H, where X is the central atom in inorganic acid. Here, subscript H(O)/H(X) indicates that in inorganic acid, the H atom is bonded to the O/X atom, while O(H)/O(X) indicates that the O atom is bonded to the H/X atom. The distance between the two H-bonded O atoms (one in H_2O and the other in acid) is denoted as r_{OO}. The $D_{O(H)}$ structure, where a H atom in H_2O interacts with the −O(H) group in the acid, is simply denoted as D_{OH}, in contrast to the D_O structure, where a H atom in H_2O interacts with a double-bond oxygen (O=) in the acid. The H-bond distance between an O atom in an acid molecule and a H atom in H_2O is denoted as r_{OH}.

There are a few geometrical isomers showing the difference only in H orientations. The energy differences and barriers between these isomers due to simple H orientations are not large. These structures are floppy, and so we have discussed mainly the low-lying energy structures. The qualitative trends are not likely to change by including the facile motions of the water molecule. In this study we focus our attention on the minimum-energy structures which are highly stable. Thus, the most stable conformer among topologically different isomers for each acid is marked in bold, and in this case the CCSD(T)/CBS interaction energies and thermodynamic quantities are evaluated.

In many cases, the central atom of an acid molecule (X) interacts with the oxygen (O) atom of a water molecule through the dispersion-driven van der Waals interaction. The van der Waals radii for N, O, P, S, Cl, Br, and I are 1.55, 1.52, 1.80, 1.80, 1.75, 1.85, and 1.98 Å, respectively.[44] If the distance between X and O (r_{XO}) is close to the sum of van der Waals radii of X and O ($r_{XO} \approx r_X + r_O$), then the notation W_{XO} is employed to denote the van der Waals interaction. In some cases, the distance between X and O is significantly shorter when the electrostatic interaction between the highly positively charged X and the negatively charged O is much stronger than the dispersion-driven van der Waals interaction. In such cases, the notation E_{XO} is used to denote the electrostatic interaction between the positively charged acid X atom and the negatively charged water O atom. We note that formation of monohydrated inorganic acids is determined by hydrogen bonding, dispersion-driven van der Waals interaction, and electrostatic interaction between the positively charged acid X atom (if any) and the negatively charged water O atom. Thus, our discussion on the r_{XO} distances is based on the van der Waals radii and the NBO charges localized on X and O. The NBO charges (q in au) of the X/Y atom will be denoted as $q_{X/Y}$. To support this analysis, we provide a more in-depth analysis. We carried out a series of symmetry adapted perturbation theory (SAPT) calculations[45] based on DFT[46,47] of monohydrated $HXO_{n=0,2}$ complexes, since the X atom in HX is negatively charged, and that in HXO is weakly charged, while that in HXO_2 or HXO_3 is positively charged. Symmetry-adapted perturbation theory (SAPT)-DFT, which takes into account the dispersion energy, provides a detailed description of molecular interactions in clusters, which are decomposed into electrostatic, induction, dispersion, and exchange parts. However, the decomposition between two specific atomic sites of molecules is not possible. Thus, the analysis is qualitatively investigated. The interaction energy is decomposed into electrostatic (E_{es}), induction (E_{ind}), dispersion (E_{disp}), and exchange repulsion (E_{exch}). However, the exchange−induction term ($E_{ind-exch}$) and exchange−dispersion term ($E_{disp-exch}$) can often been added to E_{ind} and E_{disp}, respectively, to form the effective induction ($E_{ind^*} = E_{ind} + E_{ind-exch}$) and the effective dispersion ($E_{disp^*} = E_{disp} + E_{disp-exch}$), respectively, while the two terms are extracted from E_{exch} to form the effective exchange term ($E_{exch^*} = E_{exch} - (E_{ind-exch} + E_{disp-exch})$) as described previously.[48,49]

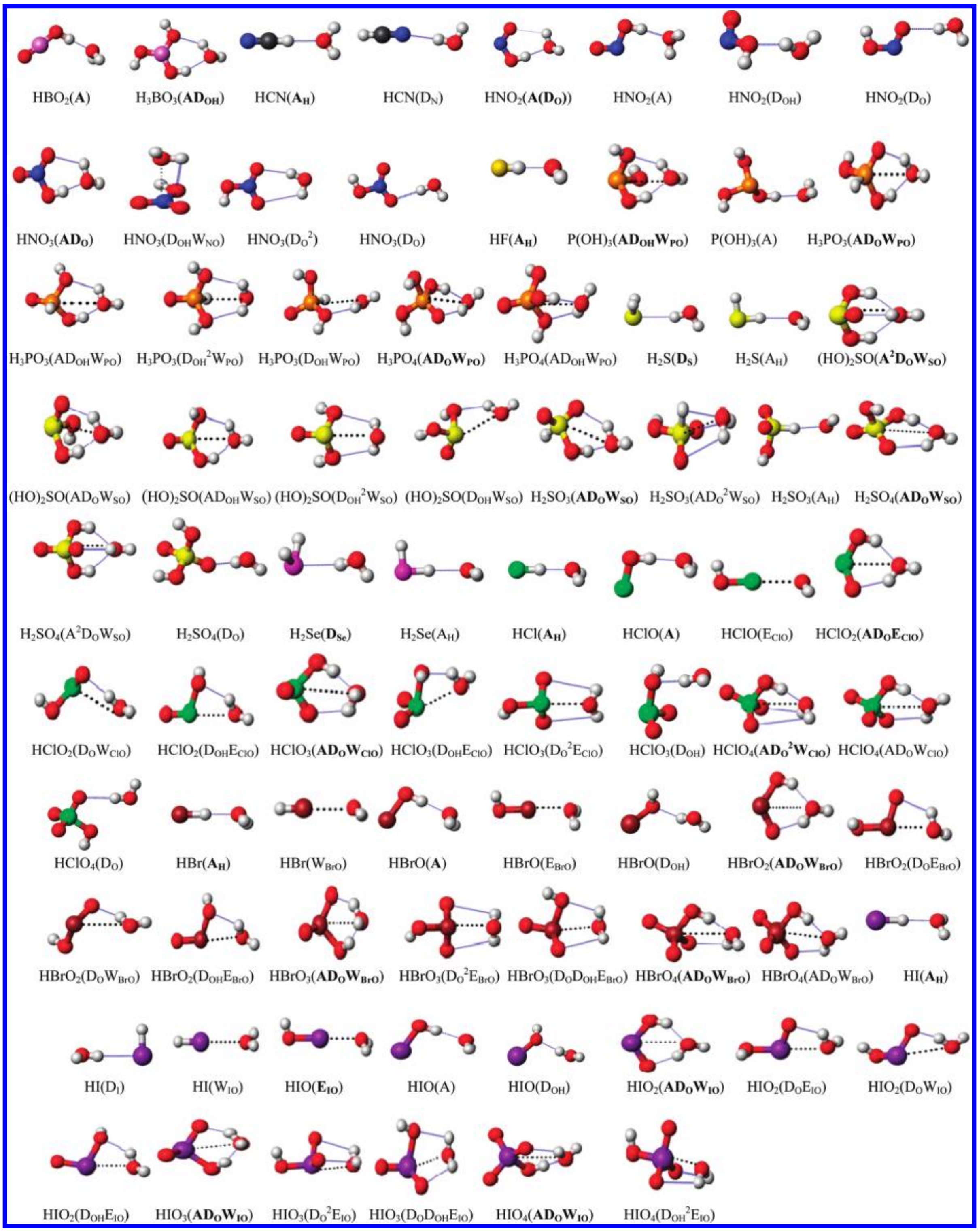

Figure 1. MP2/aVDZ optimized structures of monohydrated inorganic acids. The lowest energy structure for each chemical species is denoted in bold. Dashed lines represent hydrogen bonds. Dotted bold lines denote van der Waals or electrostatic interactions.

■ RESULTS AND DISCUSSION

Figure 1 shows various stable structures at the MP2/aVDZ level of theory. Tables 1 and 2 list MP2/aVDZ and B3LYP/aVDZ energies (ZPE-uncorrected interaction energies: ΔE_e) and structural parameters. The ZPE-corrected interaction energies (ΔE_0) and enthalpies/free energies ($\Delta H_r/\Delta G_r$ at room temperature and 1 bar) are in Supporting Information (Tables S1, S2). The geometrical parameters include the H-bond distances between acids and a water molecule (r_{OO}, r_{OH}) and the van der Waals interaction distance between the X atom of the acid and the O atom in the water molecule (r_{XO}). For the most stable structures we calculated the NBO charges at the

Table 1. MP2(B3LYP)/aVDZ Interaction Energies (ΔE_e in kJ/mol) and Selected Interatomic Distances for Various Conformers of Inorganic Acid···Water Complexes[a]

acid···water	conformer	$-\Delta E_e$	r_{OO}	r_{OH}	r_{XO}
$HBO_2\cdots H_2O$	**A**	**42.7(40.9)**	**2.71(2.70)**	**1.72(1.71)**	
$H_3BO_3\cdots H_2O$	**AD_{OH}**	**37.8(31.4)**	**2.82(2.83)**	**2.02(2.03)**	
$HCN\cdots H_2O$	**A_H**	**23.7(21.3)**		**2.05(2.04)**	
	D_N	18.5(15.2)			
$HNO_2\cdots H_2O$	**A(Do)**	**32.3(29.3)**	**2.99(3.01)**	**2.53(2.54)**	**3.39(3.38)**
	A	30.9(27.7)	2.79(2.78)	1.80(1.80)	3.25(3.34)
	D_{OH}	15.9(−)	2.96(−)	2.05(−)	3.59(−)
	D_O	10.3(7.6)	3.10(3.13)	2.15(2.17)	
$HNO_3\cdots H_2O$	**AD_O**	**43.1(40.0)**	**2.91(2.91)**	**2.39(2.39)**	**3.26(3.26)**
	$D_{OH}W_{NO}$	16.4(−)	2.87(−)	2.83(−)	2.83(−)
	$D_O{}^2$	12.3(8.2)	3.16(3.17)	2.22(2.20)	
	D_O	11.8(8.0)	3.61(3.98)	2.15(2.18)	3.61(3.98)
$P(OH)_3\cdots H_2O$	**$AD_{OH}W_{PO}$**	**41.1(31.7)**	**2.91(2.91)**	**2.07(2.07)**	**3.44(3.38)**
	A	18.2(13.9)	2.82(2.83)	1.84(1.85)	3.74(3.83)
$H_3PO_3\cdots H_2O$	**AD_OW_{PO}**	**54.8(48.7)**	**2.78(2.77)**	**1.92(1.91)**	**3.25(3.25)**
	$AD_{OH}W_{PO}$	34.9(28.1)	2.86(2.91)	2.18(2.22)	3.35(3.46)
	$D_{OH}{}^2W_{PO}$	19.5(10.9)	3.01(3.13)	2.43(2.52)	3.24(3.39)
	$D_{OH}W_{PO}$	18.7(12.3)	2.90(2.95)	2.12(2.13)	3.37(3.52)
$H_3PO_4\cdots H_2O$	**AD_OW_{PO}**	**54.9(48.3)**	**2.79(2.79)**	**1.94(1.93)**	**3.24(3.24)**
	$AD_{OH}W_{PO}$	40.0(32.3)	2.96(2.98)	2.25(2.30)	3.36(3.44)
$H_2S\cdots H_2O$	D_S	14.4(11.0)			
	A_H	13.4(9.5)		2.19(2.22)	
$(HO)_2SO\cdots H_2O$	**$A^2D_OW_{SO}$**	**49.0(39.2)**	**2.73(2.73)**	**1.99(1.98)**	**3.08(3.10)**
	AD_OW_{SO}	45.7(38.4)	2.84(2.82)	2.03(2.01)	3.27(3.31)
	$AD_{OH}W_{SO}$	37.5(28.6)	2.88(2.96)	2.19(2.29)	3.22(3.22)
	$D_{OH}{}^2W_{SO}$	18.0(9.0)	3.00(3.14)	2.45(2.51)	3.08(3.30)
	$D_{OH}W_{SO}$	15.6(10.4)	2.91(3.02)	2.13(2.06)	3.21(4.16)
$H_2SO_3\cdots H_2O$	**AD_OW_{SO}**	**52.3(46.4)**	**2.83(2.83)**	**2.09(2.09)**	**3.34(3.34)**
	$AD_O{}^2W_{SO}$	28.4(−)	3.14(−)	2.80(−)	2.93(−)
	A_H	25.4(22.0)		2.00(1.97)	
$H_2SO_4\cdots H_2O$	**AD_OW_{SO}**	**53.3(46.4)**	**2.88(2.88)**	**2.17(2.17)**	**3.30(3.33)**
	$A^2D_OW_{SO}$	47.6(37.1)	2.77(2.79)	2.18(2.20)	3.04(3.08)
	D_O	11.5(6.5)	3.03(3.06)	2.08(2.10)	
$H_2Se\cdots H_2O$	**D_{Se}**	**14.9(10.0)**			
	A_H	12.1(7.3)		2.23(2.30)	

[a] H-bond: r_{OH}; distance between two H-bonded O atoms: r_{OO}, van der Waals or electrostatic interaction: r_{XO} in Å, r_{XO} denotes the X(acid)···OH_2 distance; r_{OH} denotes either H(acid) ···OH_2 or O(acid)···HOH distance; and r_{OO} denotes the O(acid)···OH_2 distance. The (−) means that these structures do not exist at the B3LYP level of theory (lack of dispersion energy). The most stable structures are marked in bold.

MP2/aVDZ level of theory. Since the NBO charges localized on water molecule are almost identical in all the cases, we report in Table 3 the NBO charges ($q_{H(O)}$, $q_{O(H)}$, q_X) of the atoms in inorganic acids involved in H-bonding (O/H) formation and the van der Waals interaction (X−O). For the most stable conformers we also calculated ΔE_e, ΔE_0, ΔH_r, and ΔG_r at the CCSD(T)/CBS level of theory including basis set superposition error (BSSE)-corrected MP2/aVDZ, MP2/aVTZ, and CCSD(T)/aVDZ interaction energies (Table 4). In the majority of cases, B3LYP/aVDZ approach underestimates the binding energies (the absolute value of the interaction energies) as compared to the CCSD(T)/CBS results. However, it provides the proper order of conformers. Since B3LYP/aVDZ calculations are not computationally demanding, B3LYP is a good starting point for more accurate calculations by searching for many possible conformations. In some cases, to find new structures we carry out MP2 geometry optimizations. If the formation of clusters is driven by dispersion interactions, then the B3LYP method does not allow us to identify such isomers. The MP2/aVDZ approach gives reasonable values of the interaction energies, since the energy difference between CCSD(T)/CBS and MP2/aVDZ in the present systems is small in most cases, except for small iodine-containing clusters, such as HI and HIO, for which the aVDZ is not sufficient for iodine. Thus, for energy comparison between different isomers to find the most stable structures, our discussion will be based on the MP2/aVDZ ΔE_0, unless otherwise specified.

Monohydrated Inorganic Acid Complexes with B, C, N, F, P, S, Se, F, Cl, Br, and I. In the case of monohydrated metaboric acid (HBO_2), only one stable structure (A) is found. The monohydrated orthoboric acid (H_3BO_3) also forms one stable

Table 2. MP2(B3LYP)/aVDZ Interaction Energies (ΔE_e in kJ/mol) and Selected Interatomic Distances for Various Conformers of Halogen Containing Acid···Water Complexes[a]

acid···water	conformer	$-\Delta E_e$	r_{OO}	r_{OH}	r_{XO}
$HF\cdots H_2O$	**A_H**	37.8(37.7)			
$HCl\cdots H_2O$	**A_H**	25.9(23.1)			
$HClO\cdots H_2O$	**A**	33.6(30.0)	**2.78(2.78)**	**1.79(1.79)**	**3.51(3.59)**
	E_{ClO}	13.6(10.2)			2.77(2.76)
$HClO_2\cdots H_2O$	**AD_OE_{ClO}**	**46.1(41.3)**	**2.84(2.85)**	**2.03(2.02)**	**2.99(3.05)**
	D_OW_{ClO}	22.3(18.0)	2.87(2.91)	1.97(1.96)	3.28(3.57)
	$D_{OH}E_{ClO}$	21.6(11.8)	2.87(2.95)	2.17(2.29)	2.94(3.11)
$HClO_3\cdots H_2O$	**AD_OW_{ClO}**	**40.8(39.3)**	**2.96(2.92)**	**2.28(2.22)**	**3.27(3.32)**
	$D_{OH}E_{ClO}$	27.6(14.0)	2.81(2.93)	2.03(2.42)	2.91(2.97)
	$D_O{}^2E_{ClO}$	22.7(15.2)	3.15(3.17)	3.15(3.05)	2.79(2.86)
	D_{OH}	18.50(−)	2.94(−)	2.01(−)	4.08(−)
$HClO_4\cdots H_2O$	**$AD_O{}^2W_{ClO}$**	**49.3(44.4)**	**3.09(3.19)**	**2.56(2.75)**	**3.28(3.40)**
	AD_OW_{ClO}	47.0(42.7)	3.00(3.19)	2.45(2.75)	3.31(3.41)
	D_O	10.4(5.3)	3.21(3.28)	2.29(2.31)	4.01(4.18)
$HBr\cdots H_2O$	**A_H**	**22.8(19.0)**			
	W_{BrO}	8.2(3.8)			3.11(3.23)
$HBrO\cdots H_2O$	**A**	**32.3(28.0)**	**2.79(2.80)**	**1.81(1.81)**	**3.63(3.71)**
	E_{BrO}	21.3(16.6)			2.75(2.73)
	D_{OH}	18.3(−)	2.91(−)	2.02(−)	3.98(−)
$HBrO_2\cdots H_2O$	**AD_OW_{BrO}**	**48.6(41.3)**	**2.83(2.84)**	**1.98(1.99)**	**3.07(3.15)**
	D_OE_{BrO}	28.7(21.2)	2.94(2.94)	2.34(2.29)	2.83(2.85)
	D_OW_{BrO}	27.3(20.8)	2.84(2.88)	1.93(1.93)	3.33(3.62)
	$D_{OH}E_{BrO}$	26.9(15.7)	2.86(2.93)	2.22(2.30)	2.92(3.03)
$HBrO_3\cdots H_2O$	**AD_OW_{BrO}**	**48.0(43.1)**	**2.87(2.86)**	**2.10(2.07)**	**3.33(3.38)**
	$D_O{}^2E_{BrO}$	33.3(24.6)	3.11(3.13)	2.90(2.91)	2.76(2.78)
	$D_OD_{OH}E_{BrO}$	33.3(21.4)	2.97(3.02)	2.64(2.75)	2.82(2.86)
$HBrO_4\cdots H_2O$	**AD_OW_{BrO}**	**54.4(47.2)**	**3.02(3.02)**	**2.38(2.41)**	**3.29(3.43)**
	AD_OW_{BrO}	52.3(46.4)	2.93(2.91)	2.29(2.27)	3.37(3.47)
$HI\cdots H_2O$	**A_H**	**17.3(12.2)**			
	D_I	16.9(7.6)			
	W_{IO}	11.8(9.6)			3.18(3.16)
$HIO\cdots H_2O$	**E_{IO}**	**30.5(28.5)**			**2.76(2.75)**
	A	29.9(24.9)	2.83(2.84)	1.84(1.86)	3.76(3.84)
	D_{OH}	25.4(18.5)	2.88(2.90)	1.93(1.98)	3.88(4.35)
$HIO_2\cdots H_2O$	**AD_OW_{IO}**	**54.6(41.8)**	**2.78(2.82)**	**1.89(1.93)**	**3.16(3.24)**
	D_OE_{IO}	42.2(35.1)	2.82(2.80)	2.12(2.08)	2.78(2.78)
	D_OW_{IO}	37.5(28.7)	2.79(2.82)	1.84(1.87)	3.41(3.62)
	$D_{OH}E_{IO}$	35.7(24.3)	2.80(2.86)	2.11(2.18)	2.94(3.02)
$HIO_3\cdots H_2O$	**AD_OW_{IO}**	**54.7(47.6)**	**2.81(2.80)**	**1.96(1.98)**	**3.42(3.50)**
	$D_O{}^2E_{IO}$	45.7(39.1)	3.02(3.03)	2.67(2.69)	2.70(2.69)
	$D_OD_{OH}E_{IO}$	42.9(32.4)	2.89(2.94)	2.49(2.50)	2.79(2.82)
$HIO_4\cdots H_2O$	**AD_OW_{IO}**	**56.3(49.8)**	**2.89(2.92)**	**2.14(2.18)**	**3.52(3.55)**
	$D_{OH}{}^2E_{IO}$	39.5(33.4)	2.86(2.86)	2.60(2.61)	2.59(2.59)

[a] H-bond: r_{OH}; distance between two H-bonded O atoms: r_{OO}; van der Waals or electrostatic interaction: r_{XO} in Å; r_{XO} denotes the X(acid)···OH_2 distance; r_{OH} denotes either H(acid) ···OH_2 or O(acid)···HOH distance; r_{OO} denotes the O(acid)···OH_2 distance. The (−) means that these structures do not exist at the B3LYP level of theory (lack of dispersion energy). The most stable structures are marked in bold.

conformer (AD_{OH}). The H-bond length for HBO_2 (r_{OH} = 1.72 Å) is shorter than that for H_3BO_3 (r_{OH} = 2.02 Å).

The monohydrated hydrogen cyanide (HCN) forms two different stable structures. The most stable structure is A_H, which is ~6.2 kJ/mol more stable than the D_N structure. In the case of D_N conformer, the structure of −N···HO− motif is slightly bent (∠(NHO) = 176°).

In the case of monohydrated nitrous acid (HNO_2), the most stable structure $A(D_O)$ has one full H-bond and a partial H-bond (which cannot be considered as a real H-bond because the r_{OH} distance is too long (>2.5 Å) and the bond angle (∠(OHO) is too small (~109°)). Thus, this structure is denoted as $A(D_O)$. It is slightly more stable than the A conformer (by ~1.3 kJ/mol). The comparison of H-bond lengths of the $A(D_O)$ and D conformers

Table 3. NBO Charges Localized on the Lowest Energy Structure of Monohydrated Inorganic Acids at the MP2/aVDZ Level[a]

acid	structure	q_X	$q_{H(O)}$	$q_{O(H)}$	$q_{O=}$	q_H
HBO_2	A	1.46	0.57	−1.04	−1.02	
H_3BO_3	AD_{OH}	1.53	0.55	−1.06		
HCN	A_H	0.14				0.25
HNO_2	$A(D_o)$	0.51	0.53	−0.64	−0.43	
HNO_2	A	0.45	0.54	−0.66	−0.35	
HNO_3	AD_O	0.88	0.56	−0.58	−0.50	
HF	A_H	−0.63				0.60
$P(OH)_3$	$AD_{OH}W_{PO}$	1.73	0.55	−1.12		
H_3PO_3	AD_OW_{PO}	2.39	0.57	−1.11	−1.22	−0.11
H_3PO_4	AD_OW_{PO}	2.80	0.57	−1.10	−1.23	
H_2S	D_S	−0.29				0.15
H_2S	A_H	−0.32				0.18
$(HO)_2SO$	$A^2D_OW_{SO}$	1.91	0.54	−0.95	−1.08	
$(HO)_2SO$	AD_OW_{SO}	1.90	0.56	−0.99	−1.06	
H_2SO_3	AD_OW_{SO}	2.38	0.57	−0.98	−1.06	0.05
H_2SO_4	AD_OW_{SO}	2.77	0.57	−0.96	−1.03	
H_2Se	D_{Se}	−0.14				0.08
HCl	A_H	−0.35				0.32
HClO	A	0.16	0.54	−0.72		
$HClO_2$	AD_OE_{ClO}	1.05	0.55	−0.76	−0.85	
$HClO_3$	AD_OW_{ClO}	1.93	0.55	−0.79	−0.87	
$HClO_4$	$AD_O{}^2W_{ClO}$	2.61	0.56	−0.78	−0.83	
$HClO_4$	AD_OW_{ClO}	2.61	0.56	−0.78	−0.84	
HBr	A_H	−0.26				0.24
HBrO	A	0.25	0.54	−0.81		
$HBrO_2$	AD_OW_{BrO}	1.24	0.55	−0.84	−0.95	
$HBrO_3$	AD_OW_{BrO}	2.26	0.56	−0.90	−0.99	
$HBrO_4$	AD_OW_{BrO}	3.02	0.56	−0.88	−0.94	
$HBrO_4$	AD_OW_{BrO}	3.02	0.57	−0.89	−0.94	
HI	A_H	−0.11				0.09
HI	D_I	−0.04				0.05
HIO	E_{IO}	0.46				
HIO	A	0.39	0.53	−0.94		
HIO_2	AD_OW_{IO}	1.56	0.55	−0.99	−1.11	
HIO_3	AD_OW_{IO}	2.82	0.57	−1.08	−1.18	
HIO_4	AD_OW_{IO}	3.80	0.58	−1.08	−1.15	

[a] NBO charges, q, in au. Subscript X denotes the central atom in the inorganic acid; H(O)/O(H) denotes a H/O atom bonded to an O/H atom. O= denotes an O atom which is double-bonded to X (if there are more such oxygen atoms, we report the most negative NBO charge); subscript H in q_H denotes an H atom directly attached to X. The NBO charges of the monohydrated HIO are not reported. The OH group of HIO is not involved in any hydrogen bond formation. All reported NBO charges are localized on the acid.

shows that in the case of D structures the H-bond lengths are slightly shorter (by ~0.4 Å).

In the case of monohydrated nitric acid (HNO_3), the most stable conformer is AD_O. This structure looks similar to the $A(D_O)$ conformer of HNO_2 but different from it, because HNO_3 has two full H-bonds, while HNO_2 has only one full H-bond and another very weak H-bond. Thus, HNO_3 has a much stronger binding energy than HNO_2 (by ~10.5 kJ/mol). In the monohyrated HNO_3 the r_{NO} distance is shorter than that in the monohydrated HNO_2. The charge q_N localized on the N atom in HNO_3 (0.88 au) is substantially larger than the q_N of HNO_2 (0.51 au). The $D_{OH}W_{NO}$ conformer is less stable than AD_O, however, $D_{OH}W_{NO}$ is additionally stabilized by van der Waals interaction between N and O. It is important to note that the formation of the $D_{OH}W_{NO}$ structure is governed by dispersion energy. At the B3LYP level of theory, this structure cannot be found. The $D_O{}^2$ and D_O complexes are significantly less stable than the AD_O structure.

The monohydrated hydrogen fluoride (HF) and hydrogen chloride (HCl) form one stable conformer A_H.[50,51] The interaction energy of $ClH\cdots OH_2$ is ~8.7 kJ/mol smaller in magnitude than that of $FH\cdots OH_2$. In the case of HBr and HI, both A_H and W_{XO} (X = Br, I) structures exist. It is worth noting that D_X (X = F, Cl, Br) conformers are transformed to different structures during geometry optimization (D_F to A_H, D_{Cl} to A_H, and D_{Br} to W_{BrO}). The W_{XO} structure is determined by van der Waals interaction between the heavy halogen (X) and the oxygen (O) atoms of the water molecule. In the case of monoprotic acids HX (X = F, Cl, Br, and I) the charge q_H decreases with the increasing atomic number of X. The q_H localized on HF, HCl, HBr, and HI are 0.60, 0.32, 0.24, and 0.09 au, respectively, consistent with the gradual decrease in interaction energy for the monohydration phenomenon. In the case of monohydrated HI, we find an additional D_I conformer. Its binding energy is very close to the A_H structure.

In the case of phosphorous acid (H_3PO_3), there are two different topological isomers: $HP(OH)_2O$ and $P(OH)_3$. $HP(OH)_2O$ is ~15.0 kJ/mol more stable than $P(OH)_3$. When the phosphorous acid (H_3PO_3; $HP(OH)_2O$) is monohydrated, the most stable structure is AD_OW_{PO}. The structures with a water molecule acting as a donor ($D_{OH}{}^2W_{PO}$ and $D_{OH}W_{PO}$) are significantly less stable. In the case of AD_OW_{PO} structure the H-bond length r_{OH} is 1.92 Å, while in the case of $D_{OH}{}^2W_{PO}$ structure, it is significantly longer (2.43 Å). When the $P(OH)_3$ acid is monohydrated, the most stable structure is $AD_{OH}W_{PO}$. Although both acids are isomers, their structures are quite different, since the $P(OH)_3$ acid does not contain —P=O group which excludes the formation of AD_O forms.

In the case of monohydrated phosphoric acid (H_3PO_4), the most stable structure is AD_OW_{PO}, while the $AD_{OH}W_{PO}$ structure is less stable. The most stable structures of monohydrated H_3PO_3 and H_3PO_4 have similar interaction energies, because both conformers are determined by the AD_OW_{PO} motif.

For the monohydrated hydrogen sulfide (H_2S), the D_S structure is ~1 kJ/mol more stable in ΔE_e than the A_H structure. However, the relative interaction energy difference in ΔE_0 is only ~0.08 kJ/mol, then, the two structures are almost isoenergetic. The angle (122 ± 6°) between the $O-(H)\cdots O$ axis and the bisecting axis of the out-of-plane H_2O molecule in the water dimer[52−57] is in between the angle (92.5°) of the bisecting axis of the H_2S molecule with respect to the $S\cdots(H)-O$ axis in the D_S structure and the angle (146°) of the bisecting axis of the H_2O molecule with respect to the $O-(H)\cdots S$ axis in the A_H structure, because of a slightly stronger acidity for H_2S over H_2O.

The H_2SO_3 has two different isomers: sulfonic acid [$HS(OH)O_2$ (to be denoted simply as H_2SO_3)] and sulfurous acid [$(HO)_2SO$]. The sulfonic acid is ~4.6 kJ/mol more stable than the sulfurous acid. For the monohydrated sulfonic acid (H_2SO_3), the most stable conformer is AD_OW_{SO}. For the monohydrated sulfurous acid $(HO)_2SO$, the most stable structure $A^2D_OW_{SO}$ has three hydrogen bonds. The second lowest energy conformer

Table 4. BSSE-Corrected Interaction Energies (ΔE_e) at the MP2/aVTZ and CCSD(T)/aVDZ Levels of Theory Along with the CCSD(T)/CBS Thermodynamic Quantities Estimated with the MP2/aVDZ Thermal Energies[a]

		MP2	CCSD(T)	CCSD(T)/CBS				
acid···water	structure	/aVTZ	/aVDZ	$-\Delta E_e$	$-\Delta E_0$	$-\Delta H_r$	$-\Delta G_r$	T_h
$HBO_2\cdots H_2O$	A	39.5	37.8	41.3	32.4	34.2	4.5	359
$H_3BO_3\cdots H_2O$	AD_{OH}	34.0	32.6	36.4	28.9	29.0	−8.1	245
$HCN\cdots H_2O$	A_H	20.7	19.5	21.0	16.1	16.0	−7.7	236
$HNO_2\cdots H_2O$	$A(D_O)$	29.0	28.4	32.0	23.2	24.8	−9.1	225
$HNO_2\cdots H_2O$	A	29.0	28.4	30.8	22.2	22.9	−6.6	163
$HNO_3\cdots H_2O$	AD_O	39.1	39.7	43.9	34.9	36.7	0.8	298
$HF\cdots H_2O$	A_H	34.9	33.4	36.2	24.8	29.3	−0.5	289
$P(OH)_3\cdots H_2O$	$AD_{OH}W_{PO}$	36.3	35.8	41.3	30.6	33.6	−5.8	246
$H_3PO_3\cdots H_2O$	AD_OW_{PO}	51.7	49.9	57.6	46.3	50.1	9.4	347
$H_3PO_4\cdots H_2O$	AD_OW_{PO}	51.2	50.1	58.0	47.1	50.6	11.3	360
$H_2S\cdots H_2O$	D_S	11.8	10.1	11.8	5.4	5.9	−17.5	118
$H_2S\cdots H_2O$	A_H	11.1	9.6	8.6	3.2	2.9	−19.1	129
$(HO)_2SO\cdots H_2O$	$A^2D_OW_{SO}$	45.2	45.6	52.4	40.7	44.5	2.7	299
$(HO)_2SO\cdots H_2O$	AD_OW_{SO}	42.0	44.1	50.7	39.6	43.0	2.6	288
$H_2SO_3\cdots H_2O$	AD_OW_{SO}	49.9	48.1	56.4	46.2	49.3	10.6	346
$H_2SO_4\cdots H_2O$	AD_OW_{SO}	49.8	48.3	56.0	46.2	49.0	10.6	361
$H_2Se\cdots H_2O$	D_{Se}	10.8	9.0	10.8	4.7	5.0	−18.4	125
$HCl\cdots H_2O$	A_H	22.4	19.8	20.9	12.6	15.7	−12.4	220
$HClO\cdots H_2O$	A	30.8	28.4	31.9	23.1	24.6	−3.5	279
$HClO_2\cdots H_2O$	AD_OE_{ClO}	43.0	44.2	51.3	40.6	43.9	4.5	313
$HClO_3\cdots H_2O$	AD_OW_{ClO}	38.7	40.7	49.1	38.2	41.6	2.1	303
$HClO_4\cdots H_2O$	$AD_O{}^2W_{ClO}$	47.2	46.9	55.8	45.9	48.4	11.4	338
$HClO_4\cdots H_2O$	AD_OW_{ClO}	45.1	44.6	53.2	43.9	46.2	9.6	285
$HBr\cdots H_2O$	A_H	20.8	15.7	19.1	11.6	14.2	−12.8	198
$HBrO\cdots H_2O$	A	30.3	27.1	31.4	23.0	24.2	−1.6	290
$HBrO_2\cdots H_2O$	AD_OW_{BrO}	46.3	45.2	53.9	43.7	46.8	7.4	315
$HBrO_3\cdots H_2O$	AD_OW_{BrO}	46.6	44.6	54.7	43.8	47.3	7.7	306
$HBrO_4\cdots H_2O$	AD_OW_{BrO}	51.7	49.8	59.3	48.9	52.0	12.7	358
$HBrO_4\cdots H_2O$	AD_OW_{BrO}	50.4	48.3	58.0	48.3	51.2	12.8	360
$HI\cdots H_2O$	A_H	10.2	8.2	(9.3)	(3.6)	(4.9)	(−17.5)	166
$HI\cdots H_2O$	D_I	4.1	(−)	(−)	(−)	(−)	(−)	(−)
$HIO\cdots H_2O$	E_{IO}	22.1	16.6	(19.9)	(14.1)	(14.1)	(−16.7)	241
$HIO\cdots H_2O$	A	25.1	22.2	(27.2)	(19.1)	(20.1)	(−7.0)	101
$HIO_2\cdots H_2O$	AD_OW_{IO}	44.1	45.6	(50.8)	(40.6)	(43.8)	(3.9)	356
$HIO_3\cdots H_2O$	AD_OW_{IO}	49.1	47.7	(55.4)	(43.6)	(48.0)	(5.0)	328
$HIO_4\cdots H_2O$	AD_OW_{IO}	52.8	51.3	(59.7)	(49.5)	(53.0)	(14.8)	388

[a] ΔE_e, ΔE_0, ΔH_r, and ΔG_r in kJ/mol. The temperature (T_h) [K] to form a stable monohydration structure [i.e., $\Delta G(T_h) = 0$] is approximately estimated based on the harmonic frequency thermal energies. The CCSD(T)/CBS values in parentheses are approximate because only the CRENBL ECP basis set was employed for iodine without basis set expansion. In the case of monohydrated HI (D_I), it was not possible to converge CCSD(T) calculations.

AD_OW_{SO} is ~2.8 kJ/mol higher. The structures with a H-bond formed between the proton donor in the water molecule and the oxygen atom belonging to the —S═O group (AD_O) are slightly more stable than the AD_{OH} structures. The q_S of H_2SO_3 (2.38 au) is slightly larger than the q_S of $(HO)_2SO$ (1.91 au). The r_{SO} distance in monohydrated H_2SO_3 (3.34 Å) is relatively longer than that in $(HO)_2SO$ (3.08 Å).

In the case of monohydrated sulfuric acid (H_2SO_4), the most stable structure is AD_OW_{SO}, which is slightly more stable than $A^2D_OW_{SO}$. During geometry optimization, the hypothetical $AD_O{}^2$ motif is converted to the most stable AD_OW_{SO} isomer. The most stable structures of monohydrated H_2SO_3 and H_2SO_4 are very close in interaction energy because both conformers are represented by the AD_OW_{SO} motif, as noted in the case of monohydrated H_3PO_3 and H_3PO_4, which are nearly isoenergetic due to the same AD_OW_{PO} motif.

Hydrogen selenide (H_2Se) is structurally similar to the hydrogen sulfide. It forms two different stable conformers with a water molecule; the structure D_{Se} is slightly more stable than the structure A_H by ~1.7 kJ/mol, in contrast to the case of monohydrated hydrogen sulfide (H_2S) for which both structural isomers are very close in energy.

Monohydrated Inorganic Oxyacid Complexes Containing a Halogen Atom. The acids having chlorine, bromine, and iodine are significantly different from the previous cases. These heavy atoms are highly electronegative and highly polarizable.

In the case of monohydrated hypochlorous acid (HClO), the most stable conformer is A, while E_{ClO} is significantly less stable by ∼15.9 kJ/mol. The E_{ClO} structure has no hydrogen bond, but it is formed because of relatively strong electrostatic attraction between the negatively charged oxygen atom of water molecule and the positively charged chlorine atom (q_{Cl} = 0.16 au) of hypochlorous acid. In this case, the interatomic distance between Cl and O (2.77 Å) is much shorter in comparison with the sum of the van der Waals radii (3.27 Å), since the electrostatic interaction overwhelms the van der Waals interaction.

For the chlorous acid ($HClO_2$), the AD_OE_{ClO} structure is the most stable. For the monohydrated chloric acid ($HClO_3$), the AD_OW_{ClO} structure is the most stable. In the case of monohydrated perchloric acid ($HClO_4$), the $AD_O{}^2W_{ClO}$ structure is slightly more stable than the AD_OW_{ClO} structure by ∼1.8 kJ/mol. The D_O conformer is significantly less stable in comparison with $AD_O{}^2W_{ClO}$ and AD_OW_{ClO} clusters.

The monohydrated hypobromous acid (HBrO) forms conformers similar to the monohydrated hypochlorous acid. The A conformer is the most stable. The E_{BrO} conformer which has no hydrogen bond is less stable by ∼8.1 kJ/mol. The electrostatic interaction between bromine and oxygen is stronger in comparison with the E_{ClO} structure of monohydrated HClO because the q_{Br} of HBrO is 0.25 au. The monohydrated bromous acid ($HBrO_2$) forms four different molecular complexes. The most stable conformer is represented by the AD_OW_{BrO} motif. The D-type structures are significantly less stable in comparison with AD_OW_{BrO}. The bromic acid ($HBrO_3$) forms a few different structures by interacting with a water molecule; the AD_O and D types. The most stable conformer is AD_OW_{BrO}. The D conformers are significantly less stable. We also tried to find A, D_O, and D_{OH} motifs. During geometry optimization, all these conformers are converted to different structures (A to AD_OW_{BrO} and D_O as well as D_{OH} are transformed to $D_{OH}D_OE_{BrO}$). The monohydrated perbromic acid ($HBrO_4$) forms two stable AD_OW_{BrO} conformers. Both clusters are very close in energy. During geometry optimization, hypothetical A, D_O, and D_{OH} are converted to the most stable AD_OW_{BrO} form.

In the case of monohydrated hypoiodous acid (HIO), it is surprising that the most stable structure (E_{IO}) has no hydrogen bond. The E_{IO} conformer is governed by electrostatic interactions. The conformer A is slightly less stable than E_{IO} by ∼0.6 kJ/mol in ΔE_e and ∼2.9 kJ/mol in ΔE_0. In the series of HXO acids where X is Cl, Br, or I, the interaction energy difference between A and E_{XO} structures decreases with the increasing atomic mass of the halogen atom. In the case of hypoiodous acid, this order is even reversed. The relative interaction energy difference in $-\Delta E_e(-\Delta E_0)$ between A and E_{XO} for HClO, HBrO, and HIO is ∼20.0(15.9), ∼11.0(8.1), and ∼ −0.6(−2.9) kJ/mol, respectively. For the monohydrated iodous acid (HIO_2), the most stable conformer is AD_OW_{IO}. In this case, the H-bond length ($X-OH\cdots OH_2$) is slightly shorter than that in $HBrO_2$. In the case of monohydrated iodic acid (HIO_3) the AD_OW_{IO} structure is similar to those formed by $HBrO_3$. We also tried to find A, D_O, and D_{OH} conformers for the monohydrated HIO_3. During geometry optimization, A as well as D_O are transformed to the most stable AD_OW_{IO} form, and the D_{OH} structure is converted to a less stable $D_{OH}D_OE_{IO}$ isomer. For the periodic acid (HIO_4), the AD_OW_{IO} structure is the most stable. The $D_{OH}{}^2E_{IO}$ conformer is significantly less stable, however, the structure of $D_{OH}{}^2E_{IO}$ is determined by strong electrostatic interaction between I and O. During geometry optimization, hypothetical A, D_O, and D_{OH} are converted to the most stable AD_OW_{IO} form.

To verify the reliability of CRENBL ECP basis set for iodine, we carried out calculations for $HBrO_{n=0-4}\cdots H_2O$ complexes employing the CRENBL ECP basis set for the bromine atom and the aVDZ basis set for oxygen and hydrogen. The calculated values are in good agreement with the results obtained for the same complexes where all the atoms were treated with the aVDZ basis set. In general, the order in stability of conformers is preserved. However, in some cases when the energy differences between conformers are small, the order is changed. The largest binding energy difference (in terms of $-\Delta E_0$) can be observed for monohydrated $HBrO_2$ (D_OW_{BrO} motif). In this case, the energy difference is 6.9 kJ/mol. In other cases the corresponding energy differences are substantially smaller. The order is reversed for the $D_OD_{OH}E_{BrO}$ and $D_O{}^2E_{BrO}$ conformers of monohydrated $HBrO_3$. However, both structures are almost isoenergetic. For comparison, the table listing the results of $HBrO_{n=0-4}\cdots H_2O$ complexes based on the above basis sets is in the Supporting Information (Table S3).

All reported NBO charges are localized on the acid (Table 3). The NBO charges localized on hydrogen atom ($q_{H(O)}$) belonging to the −OH group are similar; the relative differences do not exceed 0.05 au. The NBO charges localized on oxygen atom ($q_{O(H)}$) are significantly different depending on different chemical species. For metaboric and orthoboric acids, $q_{O(H)}$ charges are −1.04 and −1.06 au, respectively. Those values are significantly more negative in comparison with nitrous and nitric acids (−0.64 and −0.58 au, respectively). In the case of acids containing phosphorus, the $q_{O(H)}$ charges are slightly more negative in comparison with the boric acids. The acids containing halogen atoms enable more in-depth analysis of the charge distribution. As the atomic mass of halogen atom increases, the corresponding $q_{O(H)}$ NBO charge becomes more negative. This is directly related to the NBO charge q_X of the halogen atom. As the atomic mass of X increases, the NBO charge localized on the central atom is more positive, thus the X−O bond becomes highly polarized. The q_X's are positive, except for acids which do not contain oxygen atoms. In the case of diprotic acids H_2X (X = S, Se), the q_X is more negative for the hydrogen sulfide. The sulfur is more electronegative than selenium, thus the S−H bond is more polarized. In both cases the most stable structures are D_X, thus the interaction energy is determined by a proton donor of the water molecule. In the case of monohydrated hydrogen halide acids, the most stable structure is A, since the charge distribution of HX highly affects the interaction energy.

Interaction Energies, Bond Distances, NBO Charges, and IR Red-Shifts of −OH Vibrational Modes with Respect to the Number of Oxygen Atoms (n) in $HXO_{n=0-4}$ (X = Cl, Br, I). The plots in Figure 2 are based on the minimum-energy structures [(HBO_2/A−H_3BO_3/AD_{OH}), (HNO_2/A(D_O)−HNO_3/ADo), (H_3PO_{3-4}/ADoW$_{PO}$), (H_2SO_{3-4}/ADoW$_{SO}$), (HClO/A−$HClO_{2-3}$/ADoW$_{ClO}$−$HClO_4$/ADo^{2}W$_{ClO}$), (HBrO/A−$HBrO_{2-4}$/ADoW$_{BrO}$), and (HIO/A−HIO_{2-4}/ADoW$_{IO}$)]. Figure 2a shows the relationship between binding energy [kJ/mol] and number of oxygen atoms (n) in monohydrated inorganic acids. For monohydrated $HXO_{n=0-4}$ (X = Cl, Br, I) the binding energy (the negative value of interaction energy) increases up to n = 2 and becomes almost constant for n = 2−4. In the case of n = 3, the binding energy is slightly smaller than those of n = 2,4.

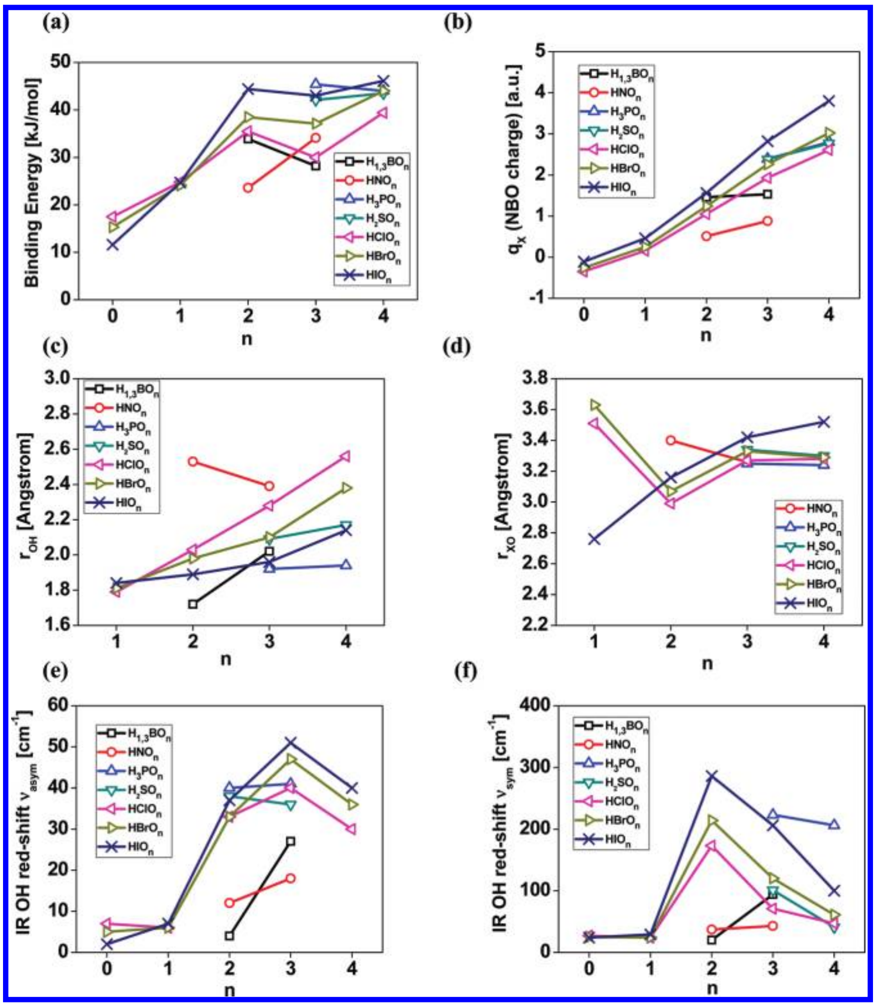

Figure 2. Plots of interaction energy [ΔE_0 in kJ/mol] (a), NBO charge [q_X in au] (b), MP2/aVDZ r_{OH} in Å (c), MP2/aVDZ r_{XO} in Å (d), IR red-shifts of −OH asymmetric (e) and asymmetric (f) vibrational frequencies in cm^{-1}, with respect to the number of oxygen atoms (n). $H_{1,3}BO_n$ denotes $HBO_{n=2}$ and $H_3BO_{n=3}$. All plots are based on the minimum-energy structures [(HBO_2/A−H_3BO_3/AD_{OH}), (HNO_2/A(D_O), HNO3/ADo), (H_3PO_{3-4}/$ADoW_{PO}$), (H_2SO_{3-4}/$ADoW_{SO}$), (HClO/A−$HClO_{2-3}$/$ADoW_{ClO}$−$HClO_4$/ADo^2W_{ClO}), (HBrO/A−$HBrO_{2-4}$/$ADoW_{BrO}$), and (HIO/A−HIO_{2-4}/$ADoW_{IO}$)]. The binding energy tends to increase up to $n = 2$ but becomes almost similar for $n = 2-4$; ν_3(OH) tends to be maximized around $n = 3$; ν_1(OH) tends to be maximized around $n = 2$. On the other hand, q_x, r_{OH}, and r_{XO} tend to increase with n for the conformations having the same type of motif. When the conformation motif changes significantly, such trends can be changed, as can be noted for the changes in the cases of (HBO_2−H_3BO_3), (HNO_{2-3}), ($HClO_{1-2}$), and ($HBrO_{1-2}$).

Figure 2b shows the relationship between the q_X NBO charges and number of oxygen atoms (n) in various inorganic acids. The graph clearly demonstrates the direct proportional relation between q_X and n (except boron containing acids). The NBO charges localized on iodine are relatively more positive than those on bromine and chlorine. The q_N charges localized on HNO_2 and HNO_3 are less positive in comparison with other inorganic acids.

Figure 2c and d shows the r_{OH} and r_{XO} distances. The relationship between r_{OH} and n and that between r_{XO} and n are similar. In both cases, for most systems, the bond length increases with n. On the other hand, the r_{OH} and r_{XO} tend to increase with n for the conformations having the same type of motif. However, when the conformation motif changes significantly, such trends can be changed, as can be noted for the changes in the cases of (HNO_{2-3}), ($HClO_{1-2}$), and ($HBrO_{1-2}$).

Figure 2e and f shows the relationship between the IR red-shifts of −OH stretching vibrational modes (asymmetric and symmetric) of the water molecule and the number of oxygen atoms (n) for the most stable monohydrated inorganic acids. The asymmetric and symmetric vibrational modes refer to the water molecule. The IR red-shifts for −OH symmetric vibrational modes are much larger than those for −OH asymmetric vibrations, as in water clusters.[58] The water symmetric OH stretch frequency [ν_3(OH)] tends to be maximized around $n = 3$; the water asymmetric OH stretch frequency [ν_1(OH)] tends to be maximized around $n = 2$. This trend is not valid in the case of (HBO_2−H_3BO_3), because the conformation motif is completely different.

For the most stable conformers, we analyze the OH stretching harmonic frequencies calculated at the MP2/aVDZ level of theory, the vibrational analysis is provided to facilitate future experiments. Figure 3 (and Tables S4 and S5 in the Supporting Information) shows the OH stretching frequencies involved in the H-bonding between the acid and the water molecule. The −OH stretching vibrational modes are important in structure identification during infrared photodissociation spectroscopy

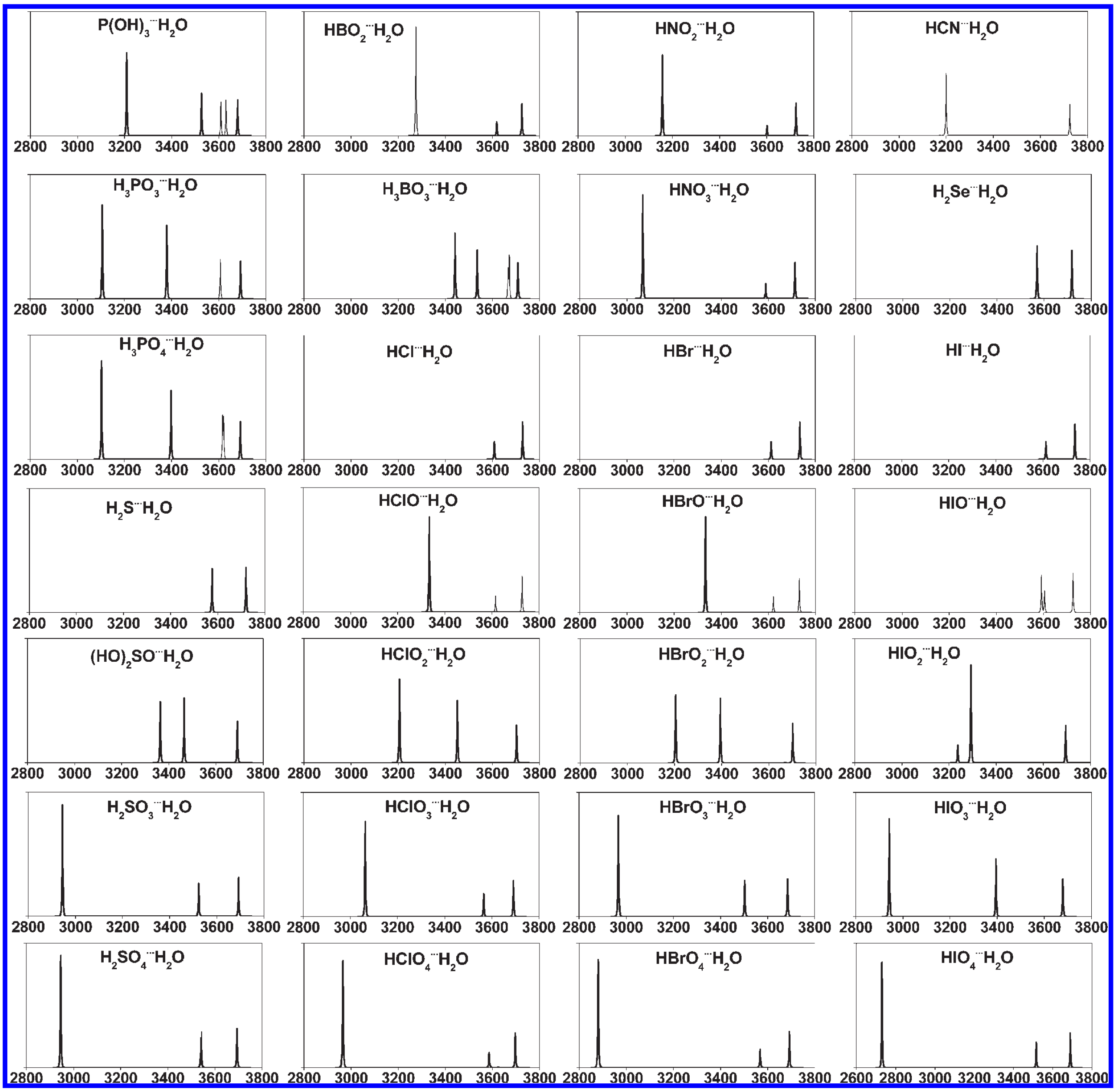

Figure 3. Predicted IR spectra of the OH anharmonic stretching frequencies (MP2/aVDZ values [cm^{-1}]). Thin lines represent stretching −OH vibrational modes of OH group which is involved in H-bond formation.

(IRPD) experiments. The IR vibrational frequencies show significant differences between acids with and without oxygen atoms. It is interesting to note the higher red-shifts of the −OH frequencies with increasing number of n for $HXO_n \cdots H_2O$, where X = Cl, Br, I. Some IR spectra exhibit coupling modes, which correspond to the simultaneous vibrations of −OH groups in inorganic acids and water molecules. The analysis of IR spectra of HClO, HBrO, and HIO clearly shows that the minimum-energy structure for HIO significantly differs from those of HClO and HBrO.

The anharmonicity of −OH stretching modes is crucial for monohydrated inorganic acids. Ab initio calculations carried out with an appropriate wave function model using the harmonic approximation can reasonably reproduce the shift of the A−H stretching band upon H-bonding. It is particularly so, if the equilibrium structure is located in a relatively deep potential well, so that both the $\upsilon = 0$ and the $\upsilon = 1$ vibrational states of the proton-stretching mode are confined within this well. However, if the equilibrium structure is found in a region of the potential energy surface, which is broad and relatively flat, or if a second region of the surface can be accessed in either the $\upsilon = 0$ or the $\upsilon = 1$ vibrational state of the proton-stretching mode, then the harmonic approximation fails. The potential energy surfaces for many monohydrated inorganic acids are relatively broad and flat. The analysis of very intensive −OH stretching modes of inorganic acids clearly shows that the differences between anharmonic and scaled harmonic frequencies (the scaling factor is 0.957)[4b] for this stretching mode in some cases are ∼100 cm^{-1}. Thus, for the most stable conformers, we calculated anharmonic frequencies based on the quartic potential surface using the Gaussian 03 suite of programs. Figure 3 contains the anharmonic

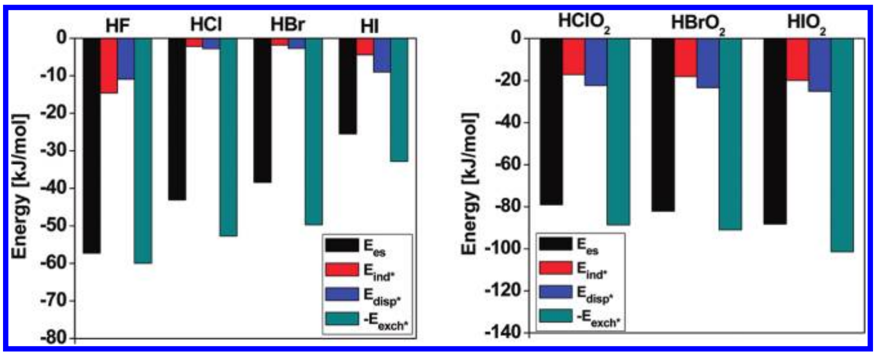

Figure 4. SAPT-DFT energy contributions [kJ/mol] for monohydrated HX (X = F, Cl, Br, I) and monohydrated HXO_2 (X = Cl, Br, I) complexes. E_{es}, E_{ind^*}, E_{disp^*}, and E_{exch^*} denote electrostatic, effective induction, effective dispersion, and effective exchange−repulsion energies, respectively.

frequencies for symmetric and asymmetric −OH stretching modes. It is important to note that scaled harmonic frequencies are usually in good agreement with anharmonic frequencies.

It is interesting to compare monohydrated $HXO_{n=2}$ complexes (as a representative case of $HXO_{n=1-3}$ for convenience's sake) with monohydrated HX complexes (X = F, Cl, Br, I). The SAPT-DFT calculations show that the electrostatic component in the monohydration energy is dominant (E_{es}) due to the H-bonding nature of both complexes (Figure 4). In the case of monohydrated HX clusters, the magnitude of electrostatic energy ($|E_{es}|$) decreases with increasing size of the halide and so is the exchange energy (E_{exch^*}) because the equilibrium distance is determined mainly by the sum of ($E_{es} + E_{exch^*}$) as long as the absolute values of induction ($|E_{ind^*}|$) and dispersion energies ($|E_{disp^*}|$) are small. In the case of F, the F···H−O distance is so short that the $|E_{disp^*}|$ is large, but the E_{exch^*} is even larger. Thus, excluding the case of F, the $|E_{disp^*}|$ increases with increasing size of the halide, but the value is not significant. On the other hand, in the case of monohydrated HXO_2 clusters the magnitude of electrostatic energy ($|E_{es}|$) increases with increasing size of the halide in contrast to the case of monohydrated HX clusters, and the dispersion and induction terms are significant. The B3LYP functional does not take into account the dispersion energy, thus in the presence of heavy X atoms, the interaction energies are smaller in magnitude than the MP2 values, and the interatomic distances are relatively longer.

In some cases, the minimum energy conformers are not stable at standard conditions. The stability of these complexes is analyzed on the basis of Gibbs free energy values (ΔG_r). In Table 4 we report T_h values for the most stable conformers. T_h corresponds to temperature at which Gibbs free energy is zero ($\Delta G(T_h) = 0$). The T_h values gives the information at what temperature a specific acid complex will have the same concentration, as the inorganic acid is no longer bound to water.

■ CONCLUDING REMARKS

We conducted a comprehensive analysis of different monohydrated inorganic acids. We carried out geometry optimization along with harmonic frequency calculations at the B3LYP and MP2 levels of theory. For each molecular system we studied all possible conformers. For inorganic acids without oxygen atoms, one or two stable conformers are found. In the case of monoprotic hydrogen halide acids, HX (X = F, Cl) one stable structure is found. For heavier halogen atoms, two stable structures are formed. The second structure does not contain H-bonds, the positively charged X atom interacts with the negatively charged oxygen atom of water molecule. The most stable monohydrated hydrogen halide is formed by the hydrogen fluoride. The monohydrated hydrogen iodide has the smallest binding energy (the negative value of interaction energy). Among monohydrated hydrogen halides, the diprotic acids H_2X (X = S, Se) form two different stable conformers. The $H_2S\cdots H_2O$ complex is slightly more stable than $H_2Se\cdots H_2O$. The metaboric acid as well as the orthoboric acid forms one stable structure, while interacting with a single water molecule. In the case of other acids, the number of possible conformers is substantially larger. In the majority of cases, AD structures are preferred. The AD structure has two H-bonds, while both acid and water are proton donors and acceptors. The inorganic acids, including chlorine, bromine, and iodine atoms, form slightly different structures. The most stable conformer in the case of $HIO\cdots H_2O$ complex has no H-bond. The structure is determined by the electrostatic interactions between iodine and oxygen. In many cases, the structures of $HXO_{n=1-4}$ (X = Cl, Br, and I) are additionally stabilized by noncovalent X···O van der Waals interactions, including the $X^+\cdots O^-$ electrostatic interactions. The hydronium cation is not formed in the case of monohydrated inorganic acids. In general, the hydronium cation which is formed by proton transfer from the acid to the water molecule is stabilized by other water molecules in the molecular system. For the most stable conformers, we calculated the interaction energy at the CCSD(T)/CBS level of theory. As compared with the CCSD(T)/CBS results, the B3LYP method highly underestimates the binding energies. The MP2/aVDZ values are not significantly different from the CCSD(T)/CBS results; the relative interaction energy differences in the present systems do not exceed ~8.2 kJ/mol. The IR spectra of acid···water systems are reported to facilitate the experiments, showing the characteristic features of H-bond interactions.

The detailed analysis of many different monohydrated inorganic acids shows that the complex formation is determined by many different factors. The geometry of the resulting complexes depends on the electronegativity of the central atom, its atomic radius, and the position of the −OH groups relative to the X═O groups. In many cases, not only the noncovalent van der Waals interactions but also the $X^+\cdots O^-$ electrostatic interactions additionally stabilize the acid···water complexes.

■ ASSOCIATED CONTENT

Ⓢ **Supporting Information.** Table S1 is the MP2(B3LYP)/aVDZ ZPE-uncorrected/ZPE-corrected interaction energies and thermodynamic properties for various conformers of monohydrated inorganic acids. Table S2 is the MP2(B3LYP)/aVDZ ZPE-uncorrected/ZPE-corrected binding energies and thermodynamic properties for various conformers of monohydrated inorganic acids containing halogen atoms. Table S3 is the MP2(B3LYP)/aVDZ ZPE-uncorrected/ZPE-corrected interaction energies and thermodynamic properties for monohydrated $HBrO_{n=0-4}$. Table S4 is the MP2/aVDZ scaled harmonic (scaling factor =0.957) and anharmonic vibrational frequencies for the most stable conformers. Table S5 is the MP2/aVDZ scaled harmonic (scaling factor =0.957) vibrational frequencies for less stable conformers. This material is available free of charges via the Internet at http://pubs.acs.org.

■ AUTHOR INFORMATION

Corresponding Author

*E-mail: kim@postech.ac.kr.

Present Addresses

‡Department of Theoretical Chemistry, Institute of Chemistry, University of Silesia, 9 Szkolna Street, 40−006 Katowice, Poland.

■ ACKNOWLEDGMENT

This work was supported by NRF (National Honor Scientist Program, WCU: R32-2008-000-10180-0) and KISTI (KSC-2011-G3-02). We thank referees for the useful comments.

■ REFERENCES

(1) (a) Stace, A. *Science* **2001**, *294*, 1292. (b) Miller, D. J.; Lisy, J. M. *J. Chem. Phys.* **2006**, *124*, 184301. (c) Lee, H. M.; Tarakeshwar, P.; Park, J. W.; Kołaski, M. R.; Yoon, Y. J.; Yi, H.-B.; Kim, W. Y; Kim, K. S. *J. Phys. Chem. A* **2004**, *108*, 2949. (d) Singh, N. J.; Park, M.; Min, S. K; Suh, S. B; Kim, K. S. *Angew. Chem., Int. Ed.* **2006**, *45*, 3795. (d) Cooper, T. E.; Carl, D. R.; Armentrout, P. B. *J. Phys. Chem. A* **2009**, *113*, 13727. (e) Carl, D. R.; Chatterjee, B. K.; Armentrout, P. B. *J. Chem. Phys.* **2010**, *132*, 044303.

(2) (a) Hurley, S. M.; Dermota, T. E.; Hydutsky, D. P.; Castleman, A. W. *Science* **2002**, *298*, 202. (b) Weber, J. M.; Kelley, J. A.; Nielsen, S. B.; Ayotte, P.; Johnson, M. A. *Science* **2000**, *287*, 2461. (c) Kołaski, M.; Lee, H. M.; Pak, C.; Kim, K. S. *J. Am. Chem. Soc.* **2008**, *130*, 103. (d) Majumdar, D.; Kim, J.; Kim, K. S. *J. Chem. Phys.* **2000**, *112*, 101. (e) Xantheas, S. S.; Dunning, T. H. J. *J. Phys. Chem.* **1994**, *98*, 13489. (f) Yates, B.; Schaefer, H. F., III; Lee, T. J.; Rice, J. E. *J. Am. Chem. Soc.* **1988**, *110*, 6327.

(3) (a) Gutberlet, A.; Schwaab, G.; Birer, O.; Masia, M.; Kaczmarek, A.; Forbert, H.; Havenith, M.; Marx, D. *Science* **2009**, *324*, 1545. (b) Odde, S.; Mhin, B. J.; Lee, K. H.; Lee, H. M.; Tarakeshwar, P.; Kim, K. S. *J. Phys. Chem. A* **2006**, *110*, 7918–7924. (c) Re, S.; Osamura, Y.; Suzuki, Y.; Schaefer, H. F., III *J. Chem. Phys.* **1998**, *109*, 973.

(4) (a) Kumar, A.; Park, M.; Huh, J. Y.; Lee, H. M.; Kim, K. S. *J. Phys. Chem. A* **2006**, *110*, 12484–12493. (b) Lee, H. M.; Tarakeshwar, P.; Kim, K. S. *J. Chem. Phys.* **2004**, *121*, 4657–4664. (c) Lee, H. M.; Kim, D.; Singh, N. J.; Kołaski, M.; Kim, K. S. *J. Chem. Phys.* **2007**, *127*, 164311.

(5) (a) Godinho, S. S. M. C.; do Couto, P. C.; Cabral, B. J. C. *J. Chem. Phys.* **2005**, *122*, 044316. (b) Odde, S.; Mhin, B. J.; Lee, H. M; Kim, K. S. *J. Chem. Phys.* **2004**, *121*, 11083. (c) Olleta, A. C.; Lee, H. M.; Kim, K. S. *J. Chem. Phys.* **2006**, *124*, 024321. (d) Singh, N. J.; Yi, H.-B.; Min, S. K.; Park, M.; Kim, K. S. *J. Phys. Chem. B* **2006**, *110*, 3808–3815. (e) Olleta, A. C.; Lee, H. M.; Kim, K. S. *J. Chem. Phys.* **2007**, *126*, 144311.

(6) (a) Orphal, J.; Kou, Q.; Tchana, F. K; Pirali, O.; Flaud, J.-M. *J. Mol. Spectrosc.* **2003**, *221*, 239. (b) Rothenberg, G.; Beadnall, R. M. H.; McGrady, J. E.; Clark, J. H. *J. Chem. Soc., Perkin Trans.* **2002**, *2*, 630. (c) Otto, A. H.; Schrader, S.; Steiger, T.; Schneider, M. *J. Chem. Soc., Faraday Trans.* **1997**, *93*, 3927.

(7) Walker, M.; Morrison, C. A.; Allan, D. R. *Phys. Rev. B* **2005**, *72*, 224106.

(8) D'Auria, R.; Turco, R. P.; Houk, K. N. *J. Phys. Chem. A* **2004**, *108*, 3756.

(9) Tao, F.-M. *J. Chem. Phys.* **1998**, *108*, 193.

(10) Nguyen, M.-T.; Jamka, A. J.; Cazar, R. A.; Tao, F.-M. *J. Chem. Phys.* **1997**, *106*, 8710.

(11) Miller, Y.; Chaban, G. M.; Gerber, R. B. *Chem. Phys.* **2005**, *313*, 213.

(12) Donaldson, D. J.; Orlando, J. J.; Amann, S.; Tyndall, G. S.; Proos, R. J.; Henry, B. R.; Vaida, V. *J. Phys. Chem. A* **1998**, *102*, 5171.

(13) Feierabenda, K. J.; Havey, D. K.; Varner, M. E.; Stanton, J. F.; Vaida, V. *J. Chem. Phys.* **2006**, *124*, 124323.

(14) Zhang, X.; Mereand, E. L.; Castleman, A. W., Jr. *J. Phys. Chem.* **1994**, *98*, 3554.

(15) Fleming, P. R.; Li, M.-G.; Rizzo, T. R. *J. Chem. Phys.* **1991**, *94*, 2425.

(16) Sinha, A.; Wal, R. L. V.; Crim, F. F. *J. Chem. Phys.* **1989**, *91*, 2929.

(17) Sinha, A.; Wal, R. L. V.; Crim, F. F. *J. Chem. Phys.* **1990**, *92*, 401.

(18) Loerting, T.; Liedl, K. R. *Proc. Natl. Acad. Sci. U.S.A.* **2000**, *97*, 8874.

(19) Larson, L. J.; Kuno, M.; Tao, F.-M. *J. Chem. Phys.* **2000**, *112*, 8830.

(20) Fiacco, D. L.; Hunt, S. W.; Leopold, K. R. *J. Am. Chem. Soc.* **2002**, *124*, 4504.

(21) Aguzzi, A.; Rossi, M. J. *Phys. Chem. Chem. Phys.* **2001**, *3*, 3707.

(22) Arstila, H.; Laasonen, K.; Laaksonen, A. *J. Chem. Phys.* **1998**, *108*, 1031.

(23) Bandy, A. R.; Ianni, J. C. *J. Phys. Chem. A* **1998**, *102*, 6533.

(24) Beichert, P.; Schrems, O. *J. Phys. Chem. A* **1998**, *102*, 10540.

(25) Re, S.; Osamura, Y.; Morokuma, K. *J. Phys. Chem. A* **1999**, *103*, 3535.

(26) Voegele, A. F.; Tautermann, C. S.; Loerting, T.; Hallbrucker, A.; Mayer, E.; Liedl, K. R. *Chem.—Eur. J.* **2002**, *8*, 5644.

(27) Bishenden, E.; Donaldson, D. J. *J. Phys. Chem. A* **1998**, *102*, 4638.

(28) Tarczay, G.; Csaszar, A. G. *J. Chem. Phys.* **2001**, *115*, 1229.

(29) Pak, C.-H; Lee, H. M.; Kim, J. C.; Kim, D.-W.; Kim, K. S. *Struct. Chem.* **2005**, *16*, 187.

(30) Alexeev, Y.; Windus, T. L.; Zhan, C. G.; Dixon, D. A. *Int. J. Quantum Chem.* **2005**, *104*, 379.

(31) Ruiz-Morales, Y.; Ziegler, T. *J. Phys. Chem. A* **1998**, *102*, 3970.

(32) Helgaker, T.; Jaszuński, M.; Ruud, K. *Chem. Rev.* **1999**, *99*, 293.

(33) Corbridge, D. E. C. *Phosphorus: An Outline of its Chemistry, Biochemistry, and Technology*; Elsevier: Amsterdam, The Netherlands, 1995, pp 677−744.

(34) Holleman, A. F.; Wiberg, E. *Inorg. Chem.*; Academic Press: San Diego, CA, 2001, pp 397−744.

(35) Malaspina, T.; Fileti, E. E.; Riveros, J. M.; Canuto, S. *J. Phys. Chem. A* **2006**, *110*, 10303.

(36) Meot-Ner, M.; Speller, C. V. *J. Phys. Chem.* **1989**, *93*, 1697.

(37) Irvine, W. M.; Morvan, D. B.; Lis, D. C.; Matthews, H. E.; Biver, N.; Criviser, J.; Davies, J. K.; Dent, W. R. F.; Gautier, D.; Godfrey, P. D.; Keene, J.; Lovel, A. J.; Owen, T. C.; Phillips, T. G.; Rauer, H.; Schloerb, F. P.; Senay, M.; Young, K. *Nature (London)* **1996**, *383*, 418.

(38) Frisch, M. J.; Trucks, G. W.; Schlegel, H. B.; Scuseria, G. E.; Robb, M. A.; Cheeseman, J. R.; Montgomery, J. A., Jr.; Vreven, T.; Kudin, K. N.; Burant, J. C.; Millam, J. M.; Iyengar, S. S.; Tomasi, J.; Barone, V.; Mennucci, B.; Cossi, M.; Scalmani, G.; Rega, N.; Petersson, G. A.; Nakatsuji, H.; Hada, M.; Ehara, M.; Toyota, K.; Fukuda, R.; Hasegawa, J.; Ishida, M.; Nakajima, T.; Honda, Y.; Kitao, O.; Nakai, H.; Klene, M.; Li, X.; Knox, J. E.; Hratchian, H. P.; Cross, J. B.; Bakken, V.; Adamo, C.; Jaramillo, J.; Gomperts, R.; Stratmann, R. E.; Yazyev, O.; Austin, A. J.; Cammi, R.; Pomelli, C.; Ochterski, J. W.; Ayala, P. Y.; Morokuma, K.; Voth, G. A.; Salvador, P.; Dannenberg, J. J.; Zakrzewski, V. G.; Dapprich, S.; Daniels, A. D.; Strain, M. C.; Farkas, O.; Malick, D. K.; Rabuck, A. D.; Raghavachari, K.; Foresman, J. B.; Ortiz, J. V.;

Cui, Q.; Baboul, A. G.; Clifford, S.; Cioslowski, J.; Stefanov, B. B.; Liu, G.; Liashenko, A.; Piskorz, P.; Komaromi, I.; Martin, R. L.; Fox, D. J.; Keith, T.; Al-Laham, M. A.; Peng, C. Y.; Nanayakkara, A.; Challacombe, M.; Gill, P. M. W.; Johnson, B.; Chen, W.; Wong, M. W.; Gonzalez, C.; Pople, J. A. *Gaussian 03*, revision C.02; Gaussian, Inc.: Wallingford, CT, 2004.

(39) Lee, S. J.; Chung, H. Y.; Kim, K. S. *Bull. Korean Chem. Soc.* **2004**, *25*, 1061.

(40) Helgaker, T.; Klopper, W.; Koch, H.; Noga, J. *J. Chem. Phys.* **1997**, *106*, 9639.

(41) Min, S. K.; Lee, E. C.; Lee, H. M.; Kim, D. Y.; Kim, D.; K. S. Kim, K. S. *J. Comput. Chem.* **2008**, *29*, 1208.

(42) Császár, A. G.; Allen, W. D.; Schaefer, H. F., III *J. Chem. Phys.* **1998**, *108*, 9751.

(43) Werner, H.-J.; Knowles, P. J.; Lindh, R.; Manby, F. R.; Schutz, M.; Celani, P.; Korona, T.; Rauhut, G.; Amos, R. D.; Bernhardsson, A.; Berning, A.; Cooper, D. L.; Deegan, M. J. O.; Dobbyn, A. J.; Eckert, F.; Hampel, C.; Hetzer, G.; Lloyd, A. W.; McNicholas, S. J.; Meyer, W.; Mura, M. E.; Nicklass, A.; Palmieri, P.; Pitzer, R.; Schumann, U.; Stoll, H.; Stone, A. J.; Tarroni, R.; Thorsteinsson, T. *MOLPRO*, a package of ab initio programs, version 2006.1; Institut für Theoretische Chemie, Universität Stuttgart: Stuttgart, Germany, 2006.

(44) Bondi, A. *J. Phys. Chem.* **1964**, *68*, 441.

(45) Jeziorski, B.; Moszyński, R.; Szalewicz, K. *Chem. Rev.* **1994**, *94*, 1887–1930.

(46) (a) Jansen, G.; Heβelmann, A. *J. Phys. Chem. A* **2001**, *105*, 646. (b) Heβelmann, A.; Jansen, G. *Chem. Phys. Lett.* **2002**, *357*, 464. (c) Heβelmann, A.; Jansen, G. *Chem. Phys. Lett.* **2002**, *362*, 319.

(47) (a) Heβelmann, A.; Jansen, G. *Chem. Phys. Lett.* **2003**, *367*, 778. (b) Heβelmann, A.; Jansen, G. *Phys. Chem. Chem. Phys.* **2003**, *5*, 5010.

(48) Lee, E. C.; Kim, D.; Jurecka, P.; Tarakeshwar, P.; Hobza, P.; Kim., K. S. *J. Phys. Chem A* **2007**, *111*, 3446–3457.

(49) Heβelmann, A.; Jansen, G.; Schütz, M. *J. Chem. Phys.* **2005**, *122*, 014103–17.

(50) Odde, S.; Mhin, B. J.; Lee., S.; Lee, H. M; Kim, K. S. *J. Chem. Phys.* **2004**, *120*, 9524.

(51) Kim, J.; Lee, H. M.; Suh, S. B.; Majumdar, D.; Kim, K. S. *J. Chem. Phys.* **2000**, *113*, 5259.

(52) Dyke, T. R; Muenter, J. S. *J. Chem. Phys.* **1974**, *60*, 2929.

(53) Dyke, T. R; J. S. Muenter, J. S. *J. Chem. Phys.* **1972**, *57*, 5011.

(54) Dyke, T. R.; Mack, K. M.; Muenter, J. S. *J. Chem. Phys.* **1977**, *66*, 498.

(55) Odutola, J. A.; Dyke, T. R. *J. Chem. Phys.* **1980**, *72*, 5062.

(56) Kim, K. S.; Mhin, B. J.; Choi, U.-S.; Lee, K. *J. Chem. Phys.* **1992**, *97*, 6649.

(57) Keutsch, F. N.; Goldman, N.; Harker, H. A.; Leforestier, C.; Saykally, R. J. *Mol. Phys.* **2003**, *101*, 3477.

(58) Lee, H. M.; Suh, S. B.; Lee, J. Y.; Tarakeshwar, P.; Kim, K. S. *J. Chem. Phys.* **2000**, *112*, 9759.